

Equilibrium analysis of zirconium carbide CVD growth

Yong Sun Won^a, Venu G. Varanasi^a, Olga Kryliouk^a, Timothy J. Anderson^{a,*},
Lisa McElwee-White^b, Rosa J. Perez^c

^aDepartment of Chemical Engineering, University of Florida, Gainesville, FL 32611-6005, USA

^bDepartment of Chemistry, University of Florida, Gainesville, FL 32611-7200, USA

^cDepartment of Materials Science and Engineering, Division of Computational Thermodynamics, Royal Institute of Technology, KTH, SE-100 44 Stockholm, Sweden

Received 8 March 2007; received in revised form 23 April 2007; accepted 22 May 2007

Communicated by G.B. Stringfellow

Available online 24 May 2007

Abstract

A chemical equilibrium study was performed to investigate the effect of growth parameters on the constitution in ZrC films grown by chemical vapor deposition (CVD). The equilibrium analysis of the Zr–C–H system demonstrated that ZrC (fcc) deposition is favorable and that a certain minimum amount of hydrogen should prevent co-deposition of elemental carbon over a wide range of temperature, pressure, and inlet C/Zr atom ratio. The results of the equilibrium analysis were compared to the phase constitution of films grown by low-pressure metalorganic CVD ($<10^{-4}$ Torr). Only carbon-rich ZrC films were grown and demonstrated the possibility of an aerosol-assisted CVD approach to stoichiometric ZrC film growth.

© 2007 Elsevier B.V. All rights reserved.

PACS: 81.05.Je; 81.15.Gh; 82–60.–s

Keywords: A1. Phase equilibria; A3. Equilibrium analysis; A3. Metalorganic chemical vapor deposition; A3. Zirconium carbide

1. Introduction

Zirconium carbide (ZrC) is a promising material for a wide range of applications. In particular, it has been proposed as an electron emitter material for field-emitter arrays (FEAs) because of its metal-like electrical conductivity ($2 \times 10^4/\Omega \text{ cm}$), high hardness (25,000 N/mm²), high melting temperature (3400 °C), correspondingly high strength at elevated temperature, and relatively low work function (4.0 eV) compared to conventional emitter materials such as Si (4.52 eV) and Mo (4.6 eV) [1–9]. The growth of ZrC, however, is not straightforward particularly by chemical vapor deposition (CVD). Although atmospheric halide CVD using zirconium tetrachloride (ZrCl₄), methane (CH₄), and hydrogen precursors has produced reasonable quality ZrC films, a relatively high growth temperature is required (1000–2000 °C), thus limiting the

list of suitable substrates. Furthermore, halide impurities are incorporated in the film and limit emitter efficiency [10,11].

An alternative approach to growth of ZrC is using the single-source metalorganic precursor tetraneopentyl zirconium (Zr[CH₂C(CH₃)₃]₄, hence referred to as ZrNp₄). This source has been successfully used to grow thin films of ZrC in the low-temperature range 300–750 °C [12–16]. The films, however, were not stoichiometric but contained excess carbon in an approximate Zr/C atom ratio 1:2 to 5. To assist in understanding this growth chemistry, a chemical equilibrium analysis of the Zr–C–H system based on the Zr–C phase diagram constructed by Guillet [17,18] was performed. Particular objectives of this study were to identify conditions that prevent carbon co-deposition and explore the effect of using solvents for delivery of low volatility ZrNp₄ as an aerosol [19]. This equilibrium analysis demonstrates the possibility of growing stoichiometric ZrC (fcc) with this precursor and the results are supported by preliminary experimental results.

*Corresponding author. Tel.: +1 352 392 0946; fax: +1 352 392 9673.

E-mail address: tim@ufl.edu (T.J. Anderson).

These results should also be useful in evaluating other metalorganic precursors, which will likely be required to meet the broad range of proposed applications of ZrC.

2. Experimental procedure

ZrC films were grown from ZrNp₄ solutions (0.0177 M in benzonitrile) on Si substrates at temperature in the range 400–600 °C. CVD growth was performed in a horizontal, cold-wall quartz reactor equipped with a graphite susceptor, radio frequency (RF) heater, and a load-lock chamber. Precursor solutions were subjected to ultrasonic nebulization, which resulted in small droplets with controlled size [19]. The feed rate of the solution was 4 mL/h (0.067 sccm) and the total amount of solution was 10 mL [20]. Hydrogen (99.999% purity) was used as carrier gas [20].

The trial of aerosol-assisted metalorganic chemical vapor deposition (AA-MOCVD) using ZrNp₄ generally had a very low growth rate, 100–150 nm/h. The films were smooth and homogeneous, and exhibited good adherence to the Si substrates. EDS analysis indicated the existence of zirconium, carbon, and oxygen. XPS spectra confirmed carbide growth with Zr 3d_{3/2}, 3d_{5/2} peak separation (carbide and oxide). XRD measurements generally failed to detect crystalline ZrC, Zr oxycarbides (having the same fcc structures with a negligible difference in lattice constant) or ZrO₂, regardless of the growth temperature, suggesting the films were amorphous. As the temperature increased, the grain size and RMS surface roughness increased as measured by AFM. Detailed characterization results have been presented elsewhere [20]. The chemical composition of the films based on AES measurements will be discussed along with the equilibrium analysis results.

3. Calculations and thermochemical properties

The thermodynamic properties for gas species were taken from the *ThermoCalc* database [21–25], while the Zr–C database suggested by the assessment of Guillermet was used to describe the condensed phase thermodynamic properties [17,18]. The following five stable condensed phases were considered in his analysis; hcp (α) phase with formula (Zr)₁(C, Va)_{0.5}, bcc (β) phase with formula (Zr)₁(C,Va)₃, fcc (γ) phase with formula (Zr)₁(C, Va)₁, graphite, and a liquid solution. All relevant gas phase species contained in the *ThermoCalc* database were included in the calculation. For the conditions of this study, the only species that exhibited a partial pressure $\geq 10^{-8}$ atm were H₂, CH₄, HCl, ZrCl₄, and C₂H₆. The gas phase species and condensed phases included in the calculation are listed in Table 1.

Guillermet [17,18] used the compound energy model (CEM) to describe the solution thermodynamics of the first three interstitial phases, while the liquid phase was treated as a random solution using the substitutional model for the excess Gibbs energy. Thermodynamic properties of the metastable carbides (α and γ phases) were estimated based

Table 1

A list of gas phase species and condensed phases included in the calculation

Gas phase species	C, C ₁₂ H ₂₆ , CCl, CClH, CClH ₂ , CClH ₃ , CCl ₂ , CCl ₂ H, CCl ₂ H ₂ , CCl ₃ , CCl ₃ H, CCl ₄ , CH, CH ₂ , CH ₃ , CH ₄ , C ₂ , C ₂ Cl, C ₂ ClH, C ₂ ClH ₃ , C ₂ ClH ₅ , C ₂ Cl ₂ , C ₂ Cl ₂ H ₂ , C ₂ Cl ₃ , C ₂ Cl ₃ H, C ₂ Cl ₃ H ₃ , C ₂ Cl ₄ , C ₂ Cl ₄ H ₂ , C ₂ Cl ₅ , C ₂ Cl ₅ H, C ₂ Cl ₆ , C ₂ H, C ₂ H ₂ , C ₂ H ₃ , C ₂ H ₄ , C ₂ H ₅ , C ₂ H ₆ , C ₃ , C ₃ H, C ₃ H ₄ , C ₃ H ₆ , C ₃ H ₈ , C ₄ , C ₄ H ₁₀ , C ₄ H ₂ , C ₄ H ₄ , C ₄ H ₆ , C ₄ H ₈ , C ₅ , C ₅ H ₈ , C ₆ ClH ₅ , C ₆ H ₆ , Cl, HCl, ZrCl, Cl ₂ , ZrCl ₂ , ZrCl ₃ , ZrCl ₄ , H, ZrH, H ₂ , Zr, Zr ₂
Condensed phases	CCl ₄ (l), C ₆ ClH ₅ (l), ZrCl ₂ (l), ZrCl ₂ (s), ZrCl ₃ (l), ZrCl ₃ (s), ZrCl ₄ (l), ZrCl ₄ (s), ZrC _{0.5} (s, α phase), ZrC ₃ (s, β phase), ZrC(s, γ phase), graphite(s), liquid solution of Zr(l) and C(l)

on the regular behavior of the vibrational entropy and other cohesive properties of transition metal carbides that had been established in his previous studies [17,18].

Thermochemical equilibrium diagrams were computed in this work using the *ThermoCalc* computational software package [25]. The results were generalized by selecting atom ratios as independent variables normalized by the inlet Zr atomic content. The calculation basis for conventional MOCVD using ZrNp₄ was Zr:C:H = 1:20:44 in addition to variable carrier H₂. For aerosol-assisted MOCVD, the basis changed considerably to Zr:C:H = 1:3856:2784 plus carrier H₂ as a result of the inclusion of the organic solvent benzonitrile (PhCN) at 0.0177 mol/L [20].

4. Results and discussion

Fig. 1 reproduces the Zr–C phase diagram proposed by Guillermet [17,18] to verify the database and to assist in the discussion of the results. The significant extent of the ZrC_x homogeneity range is evident in this phase diagram.

4.1. Phase change as a function of temperature, pressure, and inlet H/Zr ratio

The temperature–pressure deposition phase diagram is shown in Fig. 2 for three values of H/Zr atom ratio (10³, 10⁴ and 10⁵) at a fixed value of the inlet C/Zr = 20 (i.e., only ZrNp₄ and H₂ sources). It is clear that single-phase ZrC deposition is thermodynamically favorable at lower temperature and the extent of the single-phase region increases with higher pressure and higher H/Zr atom ratio. At equilibrium the carbon resides in ZrC, gas phase organics (predominantly CH₄), and under some conditions as graphite. For this specific value of C/Zr = 20, carbon co-deposition is predicted at relatively low temperature. Considering only competition between graphite and the predominant gas species CH₄ (C(graphite) + 2H₂ \leftrightarrow CH₄), it is clear that lower pressure and lower H/Zr ratio shifts the reaction towards graphite formation at fixed C/Zr. Furthermore, as the temperature increases, the negative

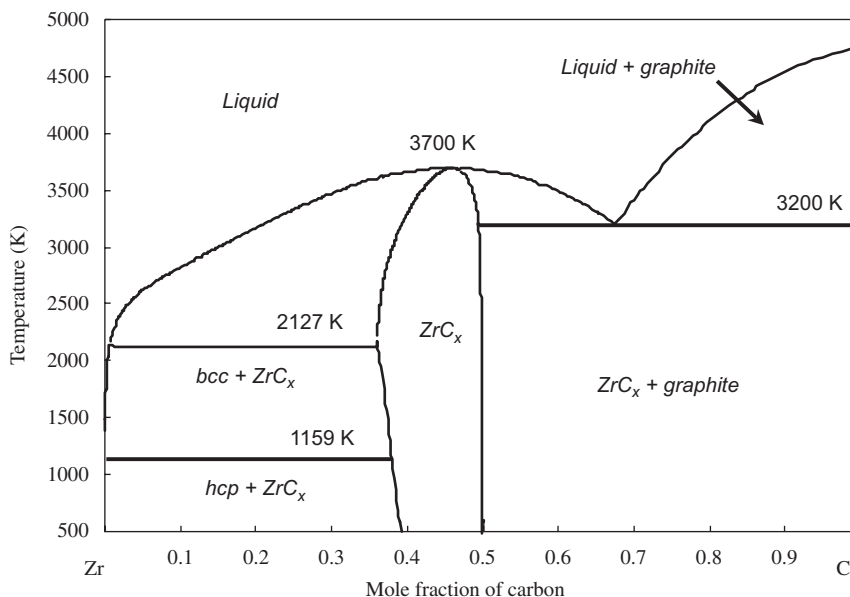


Fig. 1. The calculated Zr-C phase diagram using the assessed parameters of Guillermet [17,18].

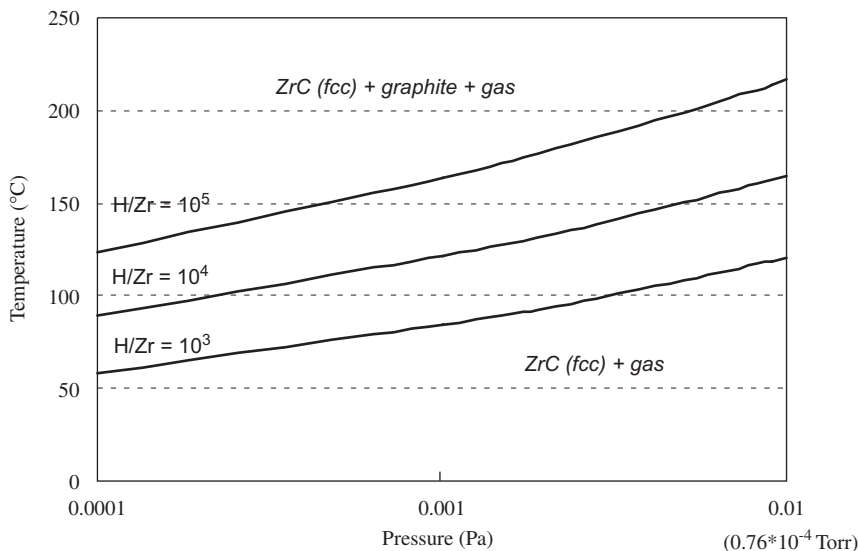
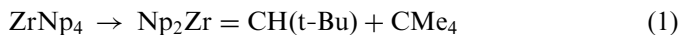


Fig. 2. CVD phase diagram showing equilibrium phases as a function of temperature and pressure for three inlet H/Zr atom ratios [inlet C/Zr = 20].

entropy change of reaction becomes more important and the equilibrium shifts to favor graphite formation.

Reaction kinetic limitations, however, are likely at low temperature. For example, it is reported that a temperature of $\sim 300^\circ\text{C}$ is required to initiate the α -hydrogen abstraction (reaction (1)), which is an important step for neopentane elimination leading to $\text{Zr}=\text{C}$ bond formation [26]. Consistent with this kinetic limitation, growth of ZrC using ZrNp_4 in AA-MOCVD at less than 400°C did not result in film growth [20]. The strategy to grow carbon-free ZrC at the kinetically required higher temperature is then to increase pressure and H/C ratio at fixed C/Zr. To grow nearly stoichiometric ZrC, however,

growth should occur near conditions that define the 2-phase ZrC + graphite boundary.



When using the aerosol delivery system a higher precursor partial pressure is possible at the expense of the Zr/C ratio since the solvent adds carbon to the system. Fig. 3 shows the equilibrium T-H/Zr deposition diagram for a fixed C/Zr = 3856 (value for the experimental study) at four reactor pressures. The CVD phase diagram shows that single-phase ZrC (fcc) deposition is possible at higher temperature by increasing the pressure and maintaining a minimum amount of hydrogen to prevent co-deposition of

graphitic carbon. Fig. 3 also shows the experimental results obtained from analysis of a set of films deposited by AA-MOCVD using ZrNp_4 at $P = 300$ Torr and inlet C/Zr ratio = 3856 [20] in the temperature range 400–600 °C. Carbide deposition along with graphite was observed in each of these films, although the equilibrium analysis predicted only single-phase ZrC . The extent of carbon deposition, however, did decrease with lower growth temperature and higher H/Zr as suggested by the equilibrium analysis. Thus, the calculations only qualitatively predicted the film phase constitution.

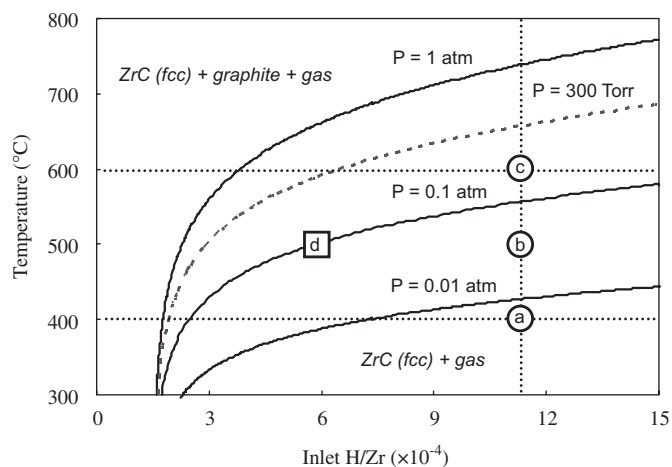


Fig. 3. CVD phase diagram showing deposited phases as a function of temperature and the inlet H/Zr ratio for four pressures [inlet $\text{C}/\text{Zr} = 3856$]. The circle and square symbols represent the growth condition of four films grown by AA-MOCVD [20] at 300 Torr and $\text{C}/\text{Zr} = 3856$: (a) $T = 400$ °C, $\text{H}/\text{Zr} = 116,000$, (b) $T = 500$ °C, $\text{H}/\text{Zr} = 116,000$, (c) $T = 600$ °C, $\text{H}/\text{Zr} = 116,000$, and (d) $T = 500$ °C, $\text{H}/\text{Zr} = 58,000$.

Fig. 4 shows the equilibrium distribution of C between the gas and condensed phases as a function of growth temperature for $\text{C}/\text{Zr} = 3856$, $\text{H}/\text{Zr} = 10^5$, and $P = 300$ Torr. It is noted that the stoichiometry of ZrC_x is nearly constant at $x = 1$ throughout the range shown in Fig. 4. Furthermore, essentially all of the Zr resides in ZrC as indicated in the inset in this figure. Below ~ 600 °C single phase and nearly stoichiometric ZrC forms and the remainder of the carbon is found in the gas phase, primarily as CH_4 . Above this temperature the graphitic carbon content in solid phase increases rapidly at the expense of carbon in the gas phase.

4.2. Phase change as a function of temperature and the inlet C/Zr ratio

In the deposition of metal carbides, a more reactive hydrocarbon is sometimes used (e.g., propane). For some sources an intermediate carbon containing species may not be reactive, and thus propane or another reactive species would be needed to provide a source of carbon. Fig. 5 shows the effect of changing the inlet carbon content for two different reactor pressures. In this calculation, the C/Zr ratio was continuously changed by adding a variable amount of C_3H_8 to a constant amount of ZrNp_4 and benzonitrile ($\text{C}/\text{Zr} = 3856$) in H_2 carrier. The H/Zr ratio necessarily varied with C/Zr ratio as required by atom conservation. As expected the addition of another carbon source lowers the 2-phase transition temperature. Based on these calculations and the experimental results that show carbon co-deposition [20], it appears that either an alternative solvent (less carbon containing or more thermally stable) should be sought or the solvent amount should be reduced to grow single-phase ZrC .

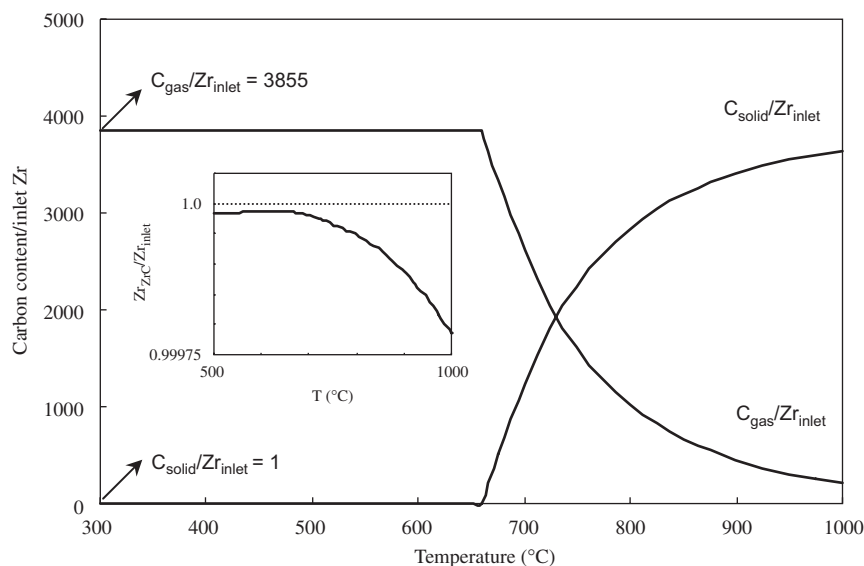


Fig. 4. Deposition efficiency as a function of growth temperature. $\text{C}_{\text{solid}}/\text{Zr}_{\text{inlet}}$ denotes the ratio of total equilibrium solid carbon ($\text{ZrC} + \text{graphite}$) to inlet Zr, and $\text{C}_{\text{gas}}/\text{Zr}_{\text{inlet}}$ represents the ratio of total equilibrium carbon in gas phase to inlet Zr. The inset shows $\text{Zr}_{\text{ZrC}}/\text{Zr}_{\text{inlet}}$. All calculations performed at $\text{C}/\text{Zr} = 3856$, $\text{H}/\text{Zr} = 10^5$, and $P = 300$ Torr.

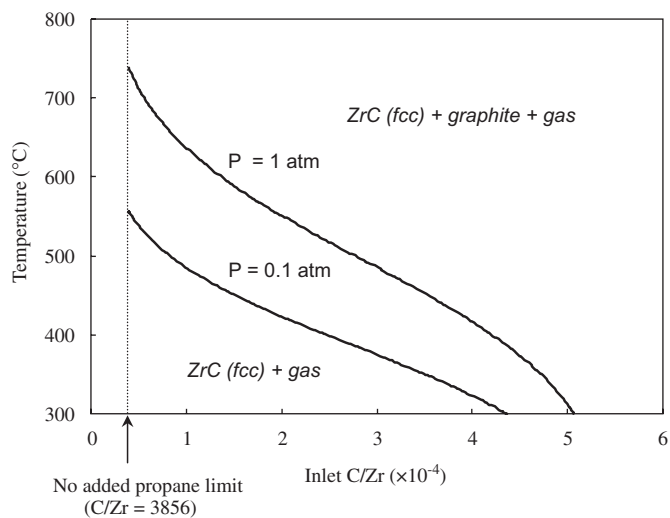


Fig. 5. CVD phase diagram showing deposited phases as a function of the inlet C/Zr ratio and temperature at 0.1 and 1.0 atm.

4.3. The addition of chlorine to the system

The growth rate of ZrC using ZrNp_4 is very low [20] likely a result of kinetic limitations in the temperature range 400–600 °C. It is suspected that physisorption on the surface of the ZrNp_4 molecule is not favorable because the tetrahedral symmetry [20] results in no permanent dipole moment. The product of α -hydrogen abstraction (see Eq. (1)), $\text{Np}_2\text{Zr}=\text{CH}(t\text{-Bu})$, is expected to be roughly trigonal planar about the Zr center, so that its dipole moment is small as well. By substituting Cl for one of the neopentyl (Np) ligands [27], results using computational chemistry (B3LYP model chemistry with a split basis set; LanL2DZ for Zr and 6-31G(d) for other elements) [28,29] suggest the dipole moments of the precursor (ZrNp_3Cl) and its α -hydrogen abstraction product ($\text{NpClZr}=\text{CH}(t\text{-Bu})$) are anticipated to be increased by a factor of three and four, respectively. Calculated dipole moments for ZrNp_3Cl and $\text{NpClZr}=\text{CH}(t\text{-Bu})$ were 2.8088 and 4.5363 D each. Chlorine is sometimes used as a transporting agent (e.g., transport of Zr as ZrCl_4) accompanied by a reducing agent (e.g., H_2) or added to the system to increase the reaction reversibility and improve the film purity. Thus, the addition of Cl to the system may improve both the kinetics as well as the equilibrium conversion. To test this latter hypothesis, equilibrium calculations were performed.

Fig. 6 shows the T-H/Zr CVD phase diagram for Zr–C–H–Cl system for two values of Cl/Zr at a fixed value of $\text{C/Zr} = 3856$ and $P = 300$ Torr. The same C/Zr ratio was retained because the loss of only four carbons by the replacement of an Np ligand with Cl is negligible. It was found that for values of the inlet Cl/Zr ratio less than 4 (see Fig. 6a), the CVD phase diagram is almost identical to the one displayed in Fig. 3 for Zr–C–H system at the same pressure, except that $\text{ZrC}(\text{fcc}) + \text{ZrCl}_4(\text{s}) + \text{graphite} + \text{gas}$ and $\text{ZrC}(\text{fcc}) + \text{ZrCl}_4(\text{s}) + \text{gas}$ phase fields appear at low temperature (< 300 °C). In contrast, the phase fields

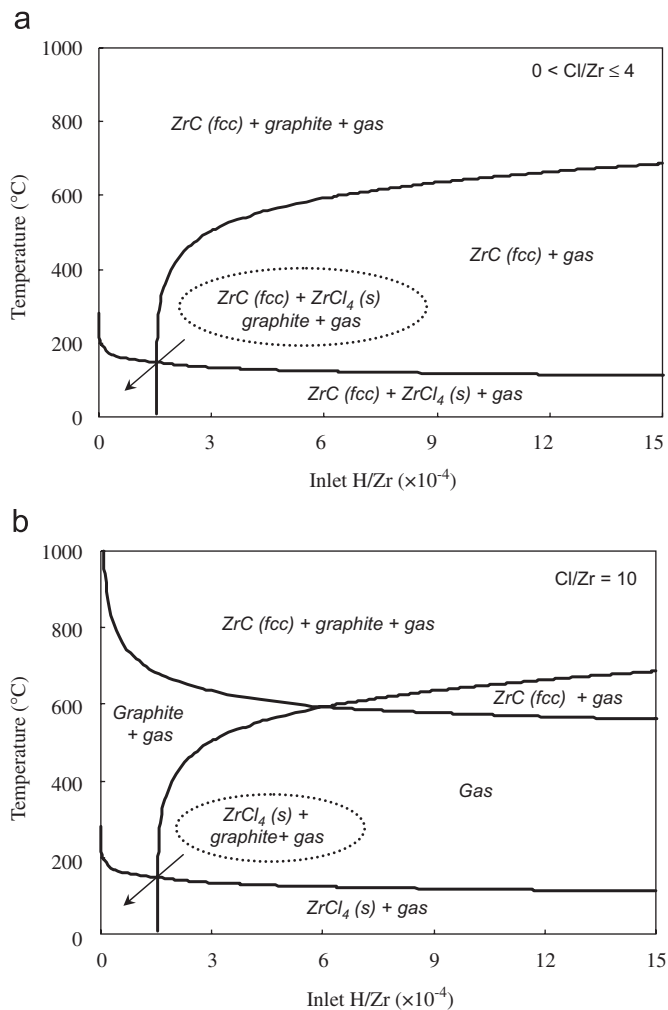


Fig. 6. CVD phase diagram showing deposited phases as a function of the inlet H/Zr ratio and temperature for two values of inlet Cl/Zr ratio. All calculations performed at $\text{C/Zr} = 3856$ and $P = 300$ Torr.

Graphite+gas and *gas* appear as the inlet Cl/Zr ratio becomes greater than 4 (see Fig. 6b) since there is sufficient Cl in the system to form $\text{ZrCl}_4(\text{g})$. It is also seen that the introduction of chlorine to the reactor to a significant proportion ($\text{Cl/Zr} > 4$) reduces the extent of the desired 2-phase $\text{ZrC}(\text{fcc}) + \text{gas}$ field. This reduction occurs by shifting the lower boundary of this 2-phase field to higher temperature, which retains the possibility of high deposition temperature. A little Cl introduction ($\text{Cl/Zr} \leq 4$) may, however, decrease a kinetic barrier to increase the rate of deposition without greatly reducing the extent of the desired single-phase ZrC domain. The use of $\text{ZrNp}_{4-x}\text{Cl}_x$ ($x = 1-3$) as a precursor is thus expected to increase growth rate with respect to ZrNp_4 , due to the greater tendency for absorption by the chlorinated complex.

The addition of HCl or a chlorine-based solvent as the Cl source is expected to reduce the equilibrium growth rate through retention of Zr in the gas phase primarily as ZrCl_4 . The effects of hydrogen and chlorine addition are different since H competes with Zr for the C while Cl competes with C for Zr. Fig. 7 illustrates this more clearly, which shows

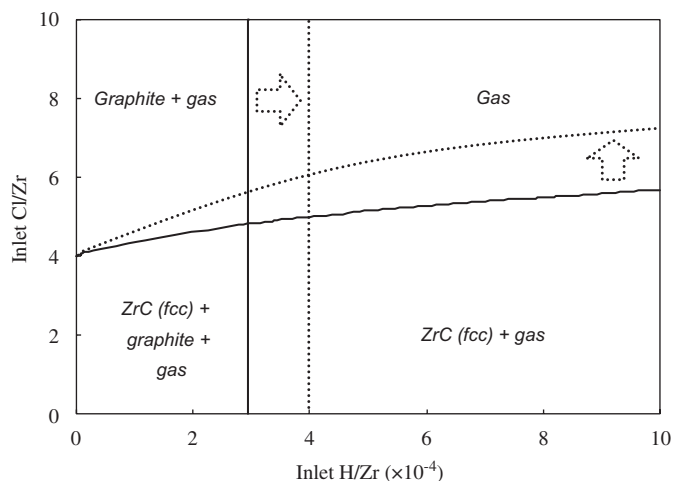


Fig. 7. CVD phase diagram showing deposited phases as a function of the inlet H/Zr and Cl/Zr ratios. All calculations performed at C/Zr = 3856, $T = 500^\circ\text{C}$, and $P = 300\text{Torr}$.

the CVD phase diagram as a function of the inlet composition (Cl/Zr and H/Zr) at fixed $P = 300\text{Torr}$, $T = 500^\circ\text{C}$, $C/Zr = 3856$. As indicated by the dotted arrows, the vertical phase transition line moves to the right and the horizontal curve (y abscissa = 4) moves upward independently, as the temperature increases. The shift to higher H/Zr of the vertical phase transition line is explained by the tendency of graphite formation over the formation of CH_4 and other hydrocarbons, while the shift to higher Cl/Zr of the horizontal phase transition line is attributed to the tendency of non-Zr containing gas species, such as HCl, over $\text{ZrCl}_4(\text{g})$ formation. It is noted that the shape of the horizontal phase transition is curved. In atmospheric halide CVD [10,11], the inlet Cl/Zr ratio is 4, so that the condition just inside the ZrC growth zone is shown in Fig. 7. ZrC growth without carbon co-deposition is possible by increasing the hydrogen carrier amount or reducing the inlet C/Zr ratio through adjustment of the CH_4 flow rate, as depicted in Figs. 7 and 5, respectively.

5. Conclusions

Equilibrium analysis supported thermodynamically the possibility of aerosol-assisted MOCVD for stoichiometric ZrC growth without carbon codeposition. The analysis suggests that co-deposition of carbon could be eliminated by ensuring the system had sufficient H and increasing the operating pressure, which relegates carbon to only vapor species. The temperature range for LP-MOCVD for stoichiometric ZrC deposition in previous experiments was not sufficiently high to overcome the activation energy for α -hydrogen abstraction, an important step to form $\text{Zr}=\text{C}$ bond by neopentane elimination. The introduction of chlorine into the existing $\text{Zr}-\text{C}-\text{H}$ system had no influence on the overall equilibrium above 400°C , the minimum temperature for overcoming kinetic limitations

of ZrNp_4 decomposition, as long as the inlet Cl/Zr ratio was less than 4.

Acknowledgments

The work is supported by the Office of Naval Research under the project number N00014-03-1-0605, Program Director Dr. Ingham A. Mack.

References

- [1] F.M. Charbonnier, J. Vac. Sci. Technol. B 16 (2) (1998) 880.
- [2] F.M. Charbonnier, W.A. Mackie, R.L. Hartman, T. Xie, J. Vac. Sci. Technol. B 19 (3) (2001) 1064.
- [3] F.M. Charbonnier, W.A. Mackie, T. Xie, P.R. Davis, Ultramicroscopy 79 (1999) 73.
- [4] W.A. Mackie, R.L. Hartman, M.A. Anderson, P.R. Davis, J. Vac. Sci. Technol. B 12 (2) (1994) 722.
- [5] W.A. Mackie, T. Xie, M.R. Matthews, B.P. Routh Jr., P.R. Davis, J. Vac. Sci. Technol. B 16 (4) (1998) 2057.
- [6] C. Spindt, C.E. Holland, P.R. Schwoebel, SPIE Proc. 3955 (2000) 151.
- [7] W.A. Mackie, T. Xie, P.R. Davis, J. Vac. Sci. Technol. B 17 (2) (1999) 613.
- [8] L.E. Toth, Transition Metal Carbides and Nitrides, Academic Press, New York, 1971.
- [9] T. Aizawa, Rep. NIRIM 81 (1994) 27.
- [10] J.A. Glass Jr., N. Palmisiano Jr., R.E. Welsh, Mater. Res. Soc. Symp. Proc. 555 (1999) 185.
- [11] H.T. Blair, D.W. Carroll, R.B. Matthews, in: M.S. El-Genk, M.D. Hoover (Eds.), Proceedings of the Eighth Symposium on Space Nuclear Power Systems, Albuquerque, NM, AIP, New York, 1991.
- [12] J.E. Parmeter, D.C. Smith, M.D. Healy, J. Vac. Sci. Technol. A 12 (4) (1994) 2107.
- [13] D.C. Smith, R.R. Rubiano, M.D. Healy, R.W. Springer, Mater. Res. Soc. Symp. Proc. 282 (1993) 642.
- [14] M.D. Healy, D.C. Smith, R.R. Rubiano, R.W. Springer, J.E. Parmeter, Mater. Res. Soc. Symp. Proc. 327 (1994) 127.
- [15] G.S. Girolami, J.A. Jensen, J.E. Gozum, D.M. Pollina, Mater. Res. Soc. Symp. Proc. 121 (1998) 429.
- [16] H. Bernt, A.Q. Zeng, H.R. Stock, P. Mayr, Surf. Coat. Technol. 74–75 (1996) 369.
- [17] A.F. Guillermet, J. Alloys Compds. 217 (1995) 69.
- [18] A.F. Guillermet, Phys. Rev. B 40 (1989) 10582.
- [19] O.J. Bchir, S.W. Johnston, A.C. Cuadra, T.J. Anderson, C.G. Ortiz, B.C. Brooks, D.H. Powell, L. McElwee-White, J. Crystal Growth 249 (1–2) (2003) 262.
- [20] Y.S. Won, Y.S. Kim, O. Kryliouk, T.J. Anderson, C.T. Sirimanne, L. McElwee-White, J. Crystal Growth 304 (2007) 324.
- [21] I. Barin, Thermochemical Data of Pure Substances, VCH, Weinheim, Germany, 1989.
- [22] O. Kubaschewski, C.B. Alcock, P.J. Spencer, Materials Thermochemistry, Pergamon Press, Oxford, UK, 1996.
- [23] A.T. Dinsdale, CALPHAD: Comput. Coupling Phase Diagrams Thermochem. 15 (1991) 317.
- [24] NIST-JANAF, in: J.M.W. Chase, (Ed.), Thermochemical Tables fourth ed., Proceedings of the American Chemical Society and the American Institute of Physics, New York, NY, 1999.
- [25] B. Sundman, B. Janson, J.O. Andersson, CALPHAD: Compt. Coupling Phase Diagrams Thermochem. 9 (1985) 153.
- [26] Y.D. Wu, Z.H. Peng, Z. Xue, J. Am. Chem. Soc. 118 (1996) 9772.
- [27] A.K. Hughes, A.J. Kingsley, J. Organomet. Chem. 539 (1–2) (1997) 109.
- [28] C.J. Cramer, Essentials of Computational Chemistry, Wiley, Chichester, UK, 2002.

- [29] M.J. Frisch, G.W. Trucks, H.B. Schlegel, G.E. Scuseria, M.A. Robb, J.R. Cheeseman, J.A. Montgomery Jr., T. Vreven, K.N. Kudin, J.C. Burant, J.M. Millam, S.S. Iyengar, J. Tomasi, V. Barone, B. Mennucci, M. Cossi, G. Scalmani, N. Rega, G.A. Petersson, H. Nakatsuji, M. Hada, M. Ehara, K. Toyota, R. Fukuda, J. Hasegawa, M. Ishida, T. Nakajima, Y. Honda, O. Kitao, H. Nakai, M. Klene, X. Li, J.E. Knox, H.P. Hratchian, J.B. Cross, V. Bakken, C. Adamo, J. Jaramillo, R. Gomperts, R.E. Stratmann, O. Yazyev, A.J. Austin, R. Cammi, C. Pomelli, J.W. Ochterski, P.Y. Ayala, K. Morokuma, G.A. Voth, P. Salvador, J.J. Dannenberg, V.G. Zakrzewski, S. Dapprich, A.D. Daniels, M.C. Strain, O. Farkas, D.K. Malick, A.D. Rabuck, K. Raghavachari, J.B. Foresman, J.V. Ortiz, Q. Cui, A.G. Baboul, S. Clifford, J. Cioslowski, B.B. Stefanov, G. Liu, A. Liashenko, P. Piskorz, I. Komaromi, R.L. Martin, D.J. Fox, T. Keith, M.A. Al-Laham, C.Y. Peng, A. Nanayakkara, M. Challacombe, P.M.W. Gill, B. Johnson, W. Chen, M.W. Wong, C. Gonzalez, J.A. Pople, Gaussian 03, Revision C.02, Gaussian Inc., Wallingford, CT, 2004, 26. Becke, A.D. *J. Chem. Phys.* 98 (1993) 1372.